# MODELING GREEN FLUORESCENT PROTEIN TRANSCRIPTION, TRANSLATION AND MODIFICATION AS A METHOD TO OBTAIN NF-κB ACTIVATION PROFILES

A Thesis

by

ALLYSON MARIE LAIBLE

Submitted to the Office of Graduate Studies of
Texas A&M University
in partial fulfillment of the requirements for the degree of

MASTER OF SCIENCE

August 2007

Major Subject: Chemical Engineering

# MODELING GREEN FLUORESCENT PROTEIN TRANSCRIPTION, TRANSLATION AND MODIFICATION AS A METHOD TO OBTAIN NF-κB ACTIVATION PROFILES

A Thesis

by

ALLYSON MARIE LAIBLE

Submitted to the Office of Graduate Studies of
Texas A&M University
in partial fulfillment of the requirements for the degree of

MASTER OF SCIENCE

Approved by:

| | |
|---|---|
| Chair of Committee, | Arul Jayaraman |
| Committee Members, | Juergen Hahn |
| | Mike McShane |
| Head of Department, | N.K. Anand |

August 2007

Major Subject: Chemical Engineering

# ABSTRACT

Modeling Green Fluorescent Protein Transcription, Translation and Modification as a Method to Obtain NF-κB Activation Profiles. (August 2007)

Allyson Marie Laible, B.S., Seattle University

Chair of Advisory Committee: Dr. Arul Jayaraman

Cellular response to inflammatory cytokines involves concerted changes in gene expression. Cytokines, such as IL-6 and TNF-α, regulate gene expression through multiple intracellular signaling pathways. The activation of transcription factors is one of the important mechanisms through which these cytokines regulate gene expression, and NF-κB is a key transcription factor that is activated by TNF-α during inflammation. In this study, we have utilized green fluorescent protein reporter cells along with fluorescence microscopy, image analysis and mechanistic modeling to determine the activation dynamics of NF-κB in H35 rat hepatoma cells upon TNF-α stimulation. NF-κB reporter cells were monitored for induction of GFP expression for 24 hours following continuous stimulation with 2.5ng/mL, 10ng/mL and 25ng/mL TNF-α. As expected, TNF-α addition resulted in a significant increase in fluorescence. Relative fluorescence profiles were generated from the fluorescence intensity data, and indicated that fluorescence increases up to 24 hours after an initial delay of approximately four hours. The fluorescence data was also used to develop a model describing significant events leading to NF-κB activation and GFP expression. In addition, a model describing

regulatable expression of GFP upon stable integration into the genome was also developed.

Comparing these two models led to the construction of a third model depicting NF-κB activation dynamics. Simulation of the model representing NF-κB activation dynamics yielded an NF- κB activation profile, which demonstrated that in the presence of constant TNF-α stimulation, there is an approximate 90 minute hour time delay followed by a rapid increase in nuclear NF-κB, that reaches a steady state value at approximately two hours.

This study establishes a method to derive NF-κB activation from reporter cell fluorescence data, and can be used to infer dynamics of activation of other transcription factors using GFP reporter cell lines.

# DEDICATION

To my family in thanks for their love and support.

# ACKNOWLEDGMENTS

I would like to extend my profound thanks to my advisor, Dr. Arul Jayaraman, and my committee members, Dr. Juergen Hahn and Dr. Mike McShane, for their guidance and support throughout the course of this research. I would like to extend my gratitude to Jacky Huang who was actively involved in this project. I would also like to thank my colleagues and the department faculty and staff for making my experience at Texas A&M University memorable and enjoyable. Finally, I would like to thank my family for their encouragement, support and love, which I would not be here without.

# TABLE OF CONTENTS

Page

CHAPTER

# LIST OF FIGURES

# LIST OF TABLES

# CHAPTER I

# INTRODUCTION

The body responds to tissue injury, infection or trauma through a coordinated sequence of events collectively termed as the inflammatory response, of which the acute phase response (APR) is an important component (Baumann and Gauldie 1994). The APR in the liver is geared towards returning the body to homeostasis and typically lasts 24-72 hours (Baumann and Gauldie 1994). One of the main features of the APR is the generation of primary cytokines that lead to the concerted changes in gene expression. These include liver specific genes that produce proteins such as albumin, $\alpha_2$-macroglobulin, serum amyloid A etc. (Baumann and Gauldie 1994). Since the liver is responsible for the production of many of the proteins and metabolites important for liver functions, changes in the expression of these genes have a significant impact on liver function (Jayaraman et al. 2000). The cytokine TNF-α plays an important role in mediating the hepatic APR, through activation of nuclear factor-kappaB (NF-κB) to elicit changes in acute phase protein (APP) gene expression.

While the APR is primarily a defense mechanism, uncontrolled or prolonged inflammation and cytokine signaling can potentially lead to chronic inflammation. For example, chronic inflammatory conditions such as septic shock, inflammatory bowl disease, atherosclerosis and hepatocellular carcinoma are all characterized by high levels

---

This thesis follows the style of Biotechnology and Bioengineering.

of TNF-α and by NF-κB activation (Barnes and Karin 1997; Wheelhouse et al. 2003; Zambon et al. 2006). Therefore, anti-inflammatory treatment strategies have targeted the regulation of cytokine signaling manipulation through signaling intermediates (Barnes and Karin 1997; Jobin et al. 1999). For modulating the expression of different transcription factors, the dynamics of expression and activation during the APR are required.

Obtaining transcription factor activation dynamics is challenging, as direct measurements of active transcription factor concentration are difficult to obtain (Barnes and Karin 1997; Moshage 1997). Typically, Western blots or mobility shift assays are used to determine activation of a transcription factor. But, these are destructive assays that require large number ($\sim$1-5 $\times 10^6$) of cells, and do not yield data on dynamic (continuous) changes of transcription factor activity. A recent approach (Wieder et al. 2005) has been to use green fluorescent protein (GFP)-based reporter cells for expression profiling. However, the data generated from such GFP reporter systems have two discrete components-the activation dynamics of the transcription factor as well as the dynamics of reporter gene expression (e.g. transcription, translation and modification). Therefore, data obtained from GFP reporter cells needs to be further analyzed to derive the dynamics of the transcription factor. This study establishes a method for extracting "true" transcription factor activation dynamics from GFP reporter cell fluorescence data using the transcription factor NF-κB as the model transcription factor.

# CHAPTER II

# BACKGROUND

## Acute Phase Response

The body responds to tissue injury, infection or trauma through a coordinated sequence of events collectively termed as the inflammatory response (Baumann and Gauldie 1994). These responses are important for returning to homeostasis and to prevent further tissue damage and infection (Baumann and Gauldie 1994). The early (24-72 hours) changes activated in response to trauma are collectively known as the APR (Moshage 1997). The APR has several features, including alterations in the expression of a number of plasma proteins known as APP. The function of APP is to return the body to homeostasis and repair tissue by confining tissue destruction, clearing harmful agents through the recruitment of immune cells and other factors to the site of the affected tissue (Han and Brasier 1997; Moshage 1997).

The liver is a principal target for the influx of inflammatory mediators because of its vital role in metabolic functions (Jayaraman et al. 2000; Moshage 1997). In response to systemic inflammation, the liver provides molecules necessary for defense via altering gene expression. (Baumann and Gauldie 1994; Moshage 1997). Acute phase proteins can be classified based on the mediator that induces them and the species in which they are produced (Moshage 1997). Type 1 acute phase proteins are induced by interleukin-1 (IL-1)-like cytokines, namely IL-1α, IL-1β, tumor necrosis factor-α (TNF-α) and tumor necrosis factor- β (TNF- β) (Moshage 1997), whereas type 2 are induced by interleukin-6 (IL-6) like cytokines (Moshage 1997). These proteins provide homeostatic,

microbicidal and phagocytic functions, contain antithrombotic properties and antiproteolytic actions, which are needed to confine protease activity at the site of inflammation (Table 1) (Moshage 1997).

**Table 1:** APP induced by type 1 and type 2 cytokines.

| Cytokine Type | APP Proteins |
|---|---|
| IL-1 like | IL-1α |
| | IL-1β |
| | TNF-α |
| | TNF-β |
| IL-6 like | Fibrinogen |
| | Heptaglobin |
| | α1-antichymotrypsin |
| | α1-antitrypsin |
| | α2-macroglobulin |

APP expression in the liver is primarily regulated through the activation of transcription factors in several signaling pathways (Baumann and Gauldie 1994). Cytokines bind to specific cell receptors causing phosporylation events that eventually lead to the activation of transcription factors. Activated transcription factors translocate into the nucleus, bind to their DNA recognition sequence in the promoter/enhancer regions of target genes and induce transcriptional activation (Moshage 1997). TNF-α is a primary cytokine regulating APP gene transcription in the liver. TNF-α stimulation of

type 1 APP genes occurs through the activation of nuclear factor-kappaB (NF-κB) (Figure 1) (Baumann and Gauldie 1994).

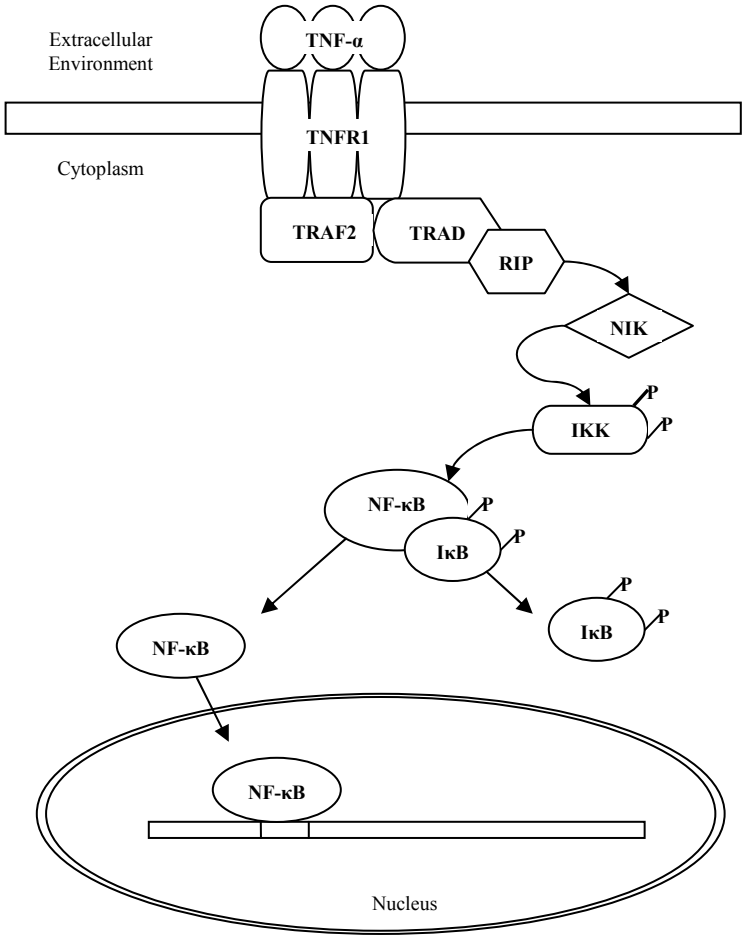


**Figure 1**. The TNF-α signaling pathway. TNF- α leads to gene expression via activation of NF-κB. TNF- α binds to its TNFR1 receptors. Aggregation of TNFR1 receptors results in the recruitment of TRAF-2 to TNFR1 by TRADD and RIP. Activated TRAF-2 activates NIK which phosphorylates the α- and β- subunits of IKK. IKK phosphorylates the α- subunit of IκB causing activation of NF-κB by the subsequent dissociation of NF-κB from IκB. NF-κB translocates to the nucleus, binds to its response elements and activates gene transcription (Henkel et al. 1993; Barnes and Karin 1997; Han and Brasier 1997; Moshage 1997; Ding et al. 1998; Chen and Ghosh 1999; Han et al. 1999; Jobin et al. 1999; Tian and Brasier 2003; Zambon et al. 2006).

TNF- α acts not only as a systemic mediator, but can also be locally produced by Kuppfer cells in the liver (Wheelhouse et al. 2003). NF-κB binding sites are present in the promoter/enhancer regions of various genes, which regulate the expression of genes that encode chemotaxis factors such as response proteins, immune receptors, other transcription factors, cell adhesion molecules, chemokines, viral proteins; inflammatory enzymes, and matrix metalloproteinases (Barnes and Karin 1997; Chen and Ghosh 1999). Activated NF-κB is therefore critical to the expression of genes that indirectly mediate the inflammatory response (Barnes and Karin 1997), as these target genes are responsible for the movement of inflammatory cells such as leukocytes, neutrophils, endothelial cells and adhesion cells to sites of tissue inflammation (Barnes and Karin 1997; Henkel et al. 1993; Smyth and Johnstone 2000).

**TNF- α Signaling and Regulation of Gene Expression Through NF-κB Activation**

Tumor necrosis factor-alpha (TNF-α) is a central pro-inflammatory cytokine produced in response to tissue injury, stress or infection, and ultimately leads to the transcription of APP defense genes (Baumann and Gauldie 1994; Ding et al. 1998; Jobin et al. 1999; Wheelhouse et al. 2003). TNF-α leads to the expression of several genes in hepatocytes through the modification and activation of latent NF-κB through a well-described signaling pathway during the APR (Han and Brasier 1997; Han et al. 1999; Henkel et al. 1993; Ros et al. 2001; Zambon et al. 2006) (Figure 1). Induction of acute phase proteins by TNF-α is mediated by TNF receptor 1 (TNFR1) (Moshage 1997; Sass et al. 2005). Upon the binding of TNF-α to its receptors, the receptors oligomerize to form trimeric structures, resulting in the intracellular assembly of their cytoplasmic signaling domains

(Moshage 1997; Smyth and Johnstone 2000; Tian and Brasier 2003). TNF receptor-associated factor 2 (TRAF-2) is recruited to the cytoplasmic portion of TNFR1 via the intermediate action of TNF receptor 1-associated death domain (TRADD) and receptor-interacting protein (RIP) (Jobin et al. 1999; Tian and Brasier 2003). TRAF-2, TRADD and RIP constitute the submembranous signaling complex (Han and Brasier 1997). Activated TRAF-2 interacts with and inherently activates the NF-κB inducing kinase (NIK) (Jobin et al. 1999). The multiprotein IκB kinase complex (IKK), composed of kinases IKK-1 and IKK-2 and regulatory subunit IKKγ, is recruited by RIP to TNFR1 (Han and Brasier 1997; Jobin et al. 1999). IKK associates with TNFR1 by IKKγ binding (Han and Brasier 1997; Jobin et al. 1999). NIK associates with and activates IKK by phosphorylating IKKα and IKKβ (Han and Brasier 1997; Jobin et al. 1999). Activated IKK is then released back into the cytosol where it tranduces the TNF-α signal and eventually activates NF-κB (Han and Brasier 1997).

**Structure and Function of NF-κB**

In unstimulated cells, NF-κB is retained in the cytoplasm in its inactive form by its inhibitor IκB (Ros et al. 2001). IκB is composed of IκBα and IκBβ subunits. NF-κB itself is a multiprotein complex composed of RelA or p65 and p50 heterodimer subunits that associate with IκB causing its sequestration in the cytoplasm (Jobin et al. 1999). These dimers contain a nuclear localization sequence (NLS) and sequences responsible for DNA binding, which are masked by the IκBα subunit of IκB (Chen and Ghosh 1999; Siebenlist et al. 1994). Rapid gene expression is achieved by the activation of NF-κB through dissociation of its inhibiting complex IκB (Barnes and Karin 1997; Ding et al.

1998; Han et al. 1999; Zambon et al. 2006). TNF-α modifies the NF-κB-IκB complex by phosphorylating and polyubiquitination of the subunits of IκBα by IKK-1 and IKK-2 (Ding et al. 1998; Han et al. 1999; Henkel et al. 1993; Jobin et al. 1999), which subsequently tags IκBα for proteolysis (Han and Brasier 1997; Tian and Brasier 2003). IκB is rapidly degraded by 26S proteosome by simultaneous proteolysis of both IκBα and IκBβ. NF-κB activation exposes the NLS, enabling NF-κB to translocate to the nucleus and bind to specific κB sequences in the response elements upstream of target genes, thereby inducing their transcription (Barnes and Karin 1997; Chen and Ghosh 1999; Jobin et al. 1999; Moshage 1997; Tian and Brasier 2003).

TNF-α not only induces proteolysis of IκB and activation of NF-κB, but also stimulates the synthesis of IκBα through NF-κB binding (Han and Brasier 1997; Siebenlist et al. 1994). Activated NF-κB induces the production of IκBα by binding to the κB elements in the promoter region of the gene coding for IκBα (Barnes and Karin 1997; Chen and Ghosh 1999). The resynthesis of IκBα is responsible for the autoregulatory feedback loop and consequent re-inhibition of NF-κB (Han and Brasier 1997; Henkel et al. 1993). Upon the synthesis of IκBα by NF-κB activation, the IκBα protein diffuses into nucleus and reassociates with the RelA dimer subunit of activated nuclear NF-κB, thereby inactivating the NLS, removing it from its target DNA, and transporting it back to the cytoplasm, thereby completely terminating NF-κB activation (Barnes and Karin 1997; Han and Brasier 1997). Transcription of APP genes therefore depends on the dynamic changes of activated NF-κB by the amount of IκBα present (Han and Brasier 1997).

This feedback regulation produces a transient response of NF-κB transcriptional activity (Siebenlist et al. 1994). In hepatocytes, this pattern consists of an early phase (15-30 minutes), followed by restoration of normal inactive levels (60 minutes), and late activation (>120 minutes) (Han and Brasier 1997).

**Effects of Chronic Inflammation**

While the APR is primarily a protective mechanism and subsides within 24-72 hours, prolonged inflammation can occur by continued cytokine signaling or inhibition of mechanisms that attenuate the inflammatory response (Baumann and Gauldie 1994; Zambon et al. 2006). In addition, chronic inflammation can be enhanced where inflammatory signaling and transcription factor activation is sustained in a positive autoregulatory feedback loop (Barnes and Karin 1997; Siebenlist et al. 1994). For example, cytokines can recruit activated immune and inflammatory cells, such as leukocytes and stromal cells, to the site of injury and induce further production of inflammatory mediators, which in turn, activate and direct additional cells to the inflamed site, thereby propagating and maintaining the inflammatory state (Barnes and Karin 1997). Therefore, the levels of cytokines in serum, in the site of inflammation, and in the liver reflect the severity of the inflammatory state (Wheelhouse et al. 2003; Zambon et al. 2006). TNF-α not only activates NF-κB, but is also produced by NF-κB induced gene expression (Siebenlist et al. 1994). Thus, this type of positive regulatory loop between cytokine generation and transcription factor activation further augments inflammation (Barnes and Karin 1997).

The persistence of cytokine signaling and transcription factor activation not only augments the inflammatory state, but may additionally influence the initiation and aggravation of inflammatory diseases, such as hepatocellular carcinoma (HCC) (Wheelhouse et al. 2003). TNF- α signaling also causes oxidative DNA damage in hepatocytes through the formation of 8-oxo-deoxyguanosine (8-oxodG) (Wheelhouse et al. 2003), which is a associated with chronic hepatitis and early hepatocarcinogenesis in the liver (Wheelhouse et al. 2003). TNF-α and NF-κB are key molecules that exaggerate HCC. Therapeutic intervention will therefore focus on controlling these molecules in order to develop treatments for inflammatory diseases such as HCC.

While the effects of chronic inflammation are well established, it is not clear which cytokines or regulatory molecules are key for the progression of acute inflammation to chronic inflammation (Baumann and Gauldie 1994). Identifying the specific molecular causalities can lead to the development of therapeutic intervention to reverse or hinder the detrimental effects of chronic inflammation (Baumann and Gauldie 1994). It is obvious, nevertheless, that anti-inflammatory treatments will target the regulation of crucial intermediaries involved in inflammatory cascades and the manipulation of cytokine signaling pathways to control APP gene expression (Barnes and Karin 1997; Jobin et al. 1999).

Because of the correlation between NF-κB and chronic inflammatory diseases, several approaches have been adopted that focus on NF-κB activation (Barnes and Karin 1997; Jobin et al. 1999). These include inhibition of synthesis, signaling and/or activity of intermediaries inhibitors (Barnes and Karin 1997; Jobin et al. 1999). While

glucocorticoids effectively inhibit NF-κB, they have also endocrine and metabolic side effects when systemically administered (Barnes and Karin 1997). Antioxidants, such as vitamins C and E and acetylcysteine have been used, but they are relatively weak inhibitors of NF-κB (Barnes and Karin 1997). Aspirin also inhibits the activation of NF-κB albeit only at relatively high concentrations (Barnes and Karin 1997).

Complete inhibition of NF-κB activation is also not desirable as the activation of NF-κB is a critical activator for protective responses (Barnes and Karin 1997). Also, NF-κB is involved in normal cell functions such as proliferation and apoptosis. Inhibition of the p65 component of NF-κB is lethal as it leads to developmental abnormalities (Barnes and Karin 1997). The knockout of the p50 component results in immune deficiencies and increased susceptibility to infection (Barnes and Karin 1997). It is therefore important to modulate NF-κB activity or partially inhibit its function for short periods.

**Regulation of Gene Expression in Reporter Cell Lines**

The response of cells to exogenous signals involves the propagation of the initiating signal through intracellular signal transducing pathways, which ultimately induce concerted changes in gene expression. The complexity of cellular pathways often makes it difficult or impossible to reliably predict the behavior of signaling intermediates (Iafolla and McMillen 2006). It is very difficult to directly measure the concentration levels of activated transcription factor proteins and determine their effect on gene expression in response to stimuli (Sanguinetti et al. 2006). To show activation of transcription factors, electrophoretic mobility shift assays or Western blots are typically

performed to monitor the specific binding between transcription factors and their DNA binding sequences in response to cytokine stimulation (Ding et al. 1998). This technique however requires harvesting a large number of cells (Ding et al. 1998; Siebenlist et al. 1994). In many cases only a small amount of the entire pool of transcription factors in the cytoplasm translocate to the nucleus despite the events that induce their activation (Subramanian and Srienc 1996). For this reason, nuclear extractions are not always optimal for determining concentrations of active transcription factors.

The recent development of green fluorescent protein (GFP) as a reporter has enabled the visualization of transcription factor activation and translocation in a small population of cells when it is transcribed in response to ligand stimulation (Subramanian and Srienc 1996). Transcription factor reporter cells contain a transcription factor DNA binding sequence upstream of a minimal promoter. GFP is not expressed when a transcription factor is not bound to its recognition sequence. Transcription factor binding results in the activation of the promoter and GFP is expression, which is visualized via fluorescence (Figure 2), and can lead to the quantification of transcription factor activation dynamics.

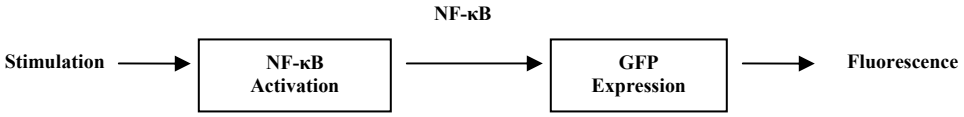


**Figure 2.** Key events leading to fluorescence in GFP reporter cell lines upon stimulation.

Expression profiling has been performed with GFP reporter cell lines for the NF-κB transcription factor (Jayaraman et al. 2000; Thompson et al. 2004; Wieder et al. 2005). However, the fluorescence profiles generated with these reporter cells include two discrete components-the dynamics of NF-κB activation in addition to the dynamics of reporter protein production. It takes a certain amount of time for a transcription factor to become activated in the presence of a signal and to translocate to its response element in the nucleus. Moreover, transcription, translation and posttranslational modification of GFP require additional time. Expression profiles generated solely from the use of reporter cell lines thus provide total dynamics of the system (e.g. stimulation, transcription factor activation, gene transcription and translation followed by fluorescence) rather than the dynamics of transcription factor activation alone. Therefore, it is necessary to decouple the contributions of reporter gene expression from the total fluorescence profiles.

**Modeling**

Mathematical modeling in combination with the utilization of reporter expression data provides a way to distinguish between the gene expression kinetics (e.g. transcription, translation and posttranscriptional modification) and the dynamics due to transcription factor activation (Sanguinetti et al. 2006; Stelling 2004). The fundamental challenge of modeling intracellular dynamics is reducing complex biological processes into mathematical equations that accurately describe the dynamics of the system. Models are generally constructed by identifying the species involved in system, formulating a set of mathematical equations that represent the interactions occurring among species,

simplifying by making assumptions, and applying known parameter values where relevant in the system of equations. Deterministic modeling is based on the formulation of a set of rate equations to describe pathway dynamics (Ullah et al. 2006). Since ordinary differential equations (ODEs) describe systematic changes over time, models generated using ODEs are advantageous for describing processes that follow rates of change (Wokenhauer et al. 2005). When quantitatively determining amounts of species present within the system, mass balances may be applied to obtain the set of ODEs (Iafolla and McMillen 2006; Ullah et al. 2006). The advantage of using mass action based models is that its terms and parameters have precise biological and relational meaning (Wokenhauer et al. 2005).

# CHAPTER III

# MATERIALS AND METHODS

## Culture Conditions

H35 NF-κB-GFP reporter cells and H35 cells constitutively expressing GFP (Wieder et al. 2005) were maintained in Dulbecco's Modified Eagle's Medium (DMEM) (Hyclone, Logan, UT) supplemented with 10% fetal bovine serum, 200U/ml penicillin and 200μg/mL streptomycin (Hyclone, Logan, UT). Cells were grown in a T-25 tissue culture flask (Beckton Dickenson Labware, Franklin Lakes, NJ) in a 5% $CO_2$ humidified incubator at 37ºC. Routine propagation of reporter cells was done using standard protocols (ATCC, Manassas, VA).

## NF-κB Stimulation Experiments

H35 NF-κB-GFP reporter cells and H35 cells expressing constitutive GFP were seeded in 6-well plates (Corning Incorporated, Corning, NJ) at a density of approximately $5 \times 10^6$ cells/well. Cells were seeded in phenol red free DMEM (Hyclone, Logan, UT) to minimize autofluorescence from phenol red. In a single experiment, cells were exposed to (2.5ng/mL,10ng/mL or 25ng/mL) TNF-α (Biosource International Inc., Camarillo CA) at 60% confluency for 24 hours and the GFP expression monitored by fluorescence microscopy. The fluorescence of H35 cells expressing constitutive GFP was measured in the absence of stimulation for 14 hours.

**Fluorescence Microscopy and Analysis**

Fluorescence microscopy was performed using a Zeiss Axiovert 200 Motorizedfluorescence microscope (Zeiss, Thornwood NY). Phase contrast and fluorescence images for three positions per well were taken every hour over the duration of the experiment. Comparison of the fluorescence intensity values for H35 NF-κB-GFP reporter cells under continual stimulation of TNF-α and H35 cells constitutively expressing GFP was carried out by image analysis in MATLAB. The contrast, brightness, and gamma values for the H35 NF-κB-GFP reporter cell images were set to 100, 16, and 1 respectively. The contrast display parameter applies a scale factor known as the gain to the colored light signals, which affects the intensity. In general, the higher the contrast value, the higher the gain applied, and the higher the intensity. Display parameters were not always consistent from image to image, resulting in fluorescence intensity enhancement. Since intensity values should depend on GFP accumulation, the display parameters of the constitutive GFP images were unified to the display parameters of the NF-κB-GFP reporter images using Equation (1), where $I_{unified}$ is the unified intensity of image $i$ when the contrast display parameter is set to 16, $I_i$ is the intensity of image $i$ at a contrast value of $C_i$.

$$I_{unified} = I_i \frac{16}{C_i} \tag{1}$$

Background regions were identified by the area of cells in phase contrast images. Cell regions were then identified and extracted from background regions. The average intensity per position was determined by calculating and averaging the fluorescence

intensities of each cell region. Mean fluorescence intensities per well were ascertained by averaging the position intensities for each well. Relative intensities were furthermore determined by subtracting the average intensities of the control images from the average fluorescence intensities per well in order to correct for medium, device fluorescence, fluorescence fluctuations and nonuniformities, and baseline levels of GFP. It is known that NF-κB is constitutively active and involved in normal cell function, therefore basal fluorescence is present even in the absence of stimulation although at minimal levels (Wieder et al. 2005). Expression profiles were then generated by plotting the relative intensities verses time.

# CHAPTER IV

# RESULTS AND DISCUSSION

## Inducible GFP Expression in NF-κB-GFP Reporter Cells

The activation dynamics of NF-κB was determined in H35 rat hepatoma cells upon TNF-α activation using a GFP reporter cell line (Wieder et al. 2005).

In the absence of TNF-α stimulation, NF-κB is present in its inactive form bound to IκB in the cytoplasm, no GFP expression and fluorescence are observed. Upon addition of TNF-α, NF-κB is activated, translocates to the nucleus, binds to its response elements upstream of the promoter of the reporter plasmid and initiates GFP expression. This regulation is shown in Figure 3.

Reporter cells were seeded in a 6-well plate at a density of approximately $5 \times 10^6$ cells/well in phenol red free DMEM to minimize autofluorescence and grown in a 5% $CO_2$ humidified environment, at 37˚C. Cultured NF- κB-GFP H35 reporter cells (approximately 60% confluent) were exposed to 2.5ng/mL,10ng/mL or 25ng/mL of TNF-α and the fluorescence was monitored over 24 hours by fluorescence microscopy. A TNF-α concentration of 10ng/mL was utilized as it has previously been used for NF-

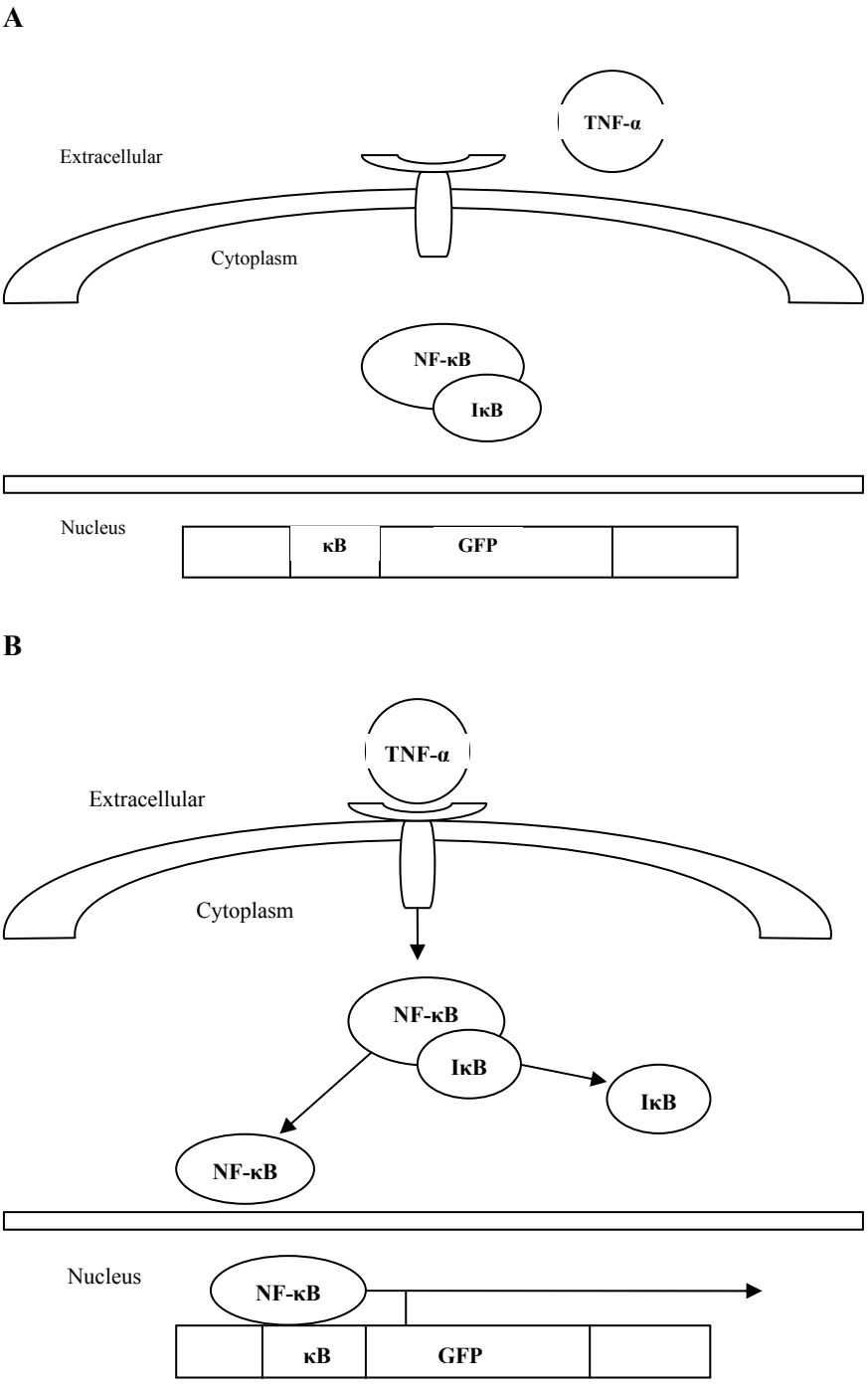


**Figure 3.** Workings of the NF-κB reporter system. **A:** Unstimulated cells do not have NF-κB binding and GFP expression. **B:** Reporter cells stimulated with TNF-α leads to gene expression via activation of NF-κB.

κB-GFP reporter cell lines (Thompson et al. 2004; Wieder et al. 2005). 2.5ng/mL and 25ng/mL TNF-α were utilized to illustrate a difference in GFP expression for a ten fold difference in TNF-α concentration. In this way, a broad range of TNF-α concentrations was used to obtain fluorescence intensities. Relative fluorescence intensities were determined and expression profiles were generated by image analysis as described in Materials and Methods in Chapter III. Figure 4 shows time-lapse phase contrast and fluorescence images taken after TNF-α stimulation, and these images show a strong increase in fluorescence upon TNF-α stimulation. The relative fluorescence profiles (Figure 5) for TNF-α addition showed approximately a four-hour time delay for cells exposed to 25ng/ml and 10ng/ml TNF-α with a similar maximum fluorescence observed at t=24 hours. Cells stimulated with 2.5ng/mL TNF-α demonstrated relatively lower GFP intensities than cells stimulated with 25ng/mL and 10ng/mL of TNF-α indicating the existence of a dose dependence in the response to TNF-α stimulation. Also, cells stimulated with 2.5ng/mL TNF-α do not show a four-hour time delay since the fluorescence images generated for these early time points were too bright to obtain intensities through image analysis. The profiles in Figure 5 suggest no significant differences between late and early time point fluorescence intensities (e.g. t=8hrs and t= 12hrs) since there is a large uncertainty associated with the intensity values. Performing image analysis where images are taken at shorter time points over 24 hours may lead to the decrease in the uncertainty in fluorescence intensity values, which may provide the ability for better model fitting. However, the profiles show similar dynamics, which in general, can be described by a similar model type.

The concentrations of TNF-α used in this study are comparable to what has been reported for normal murine plasma (~6ng/mL) (Wheelhouse et al. 2003). The intra-hepatic levels are speculated to be even higher than serum levels due to the local production of TNF-α by Kupffer cells (Wheelhouse et al. 2003). Thus, the concentration of TNF-α used in the current study, is physiologically relevant.

**Constitutive GFP Expression in H35 Cells**

H35 cells constitutively expressing GFP under the control of the CMV promoter were

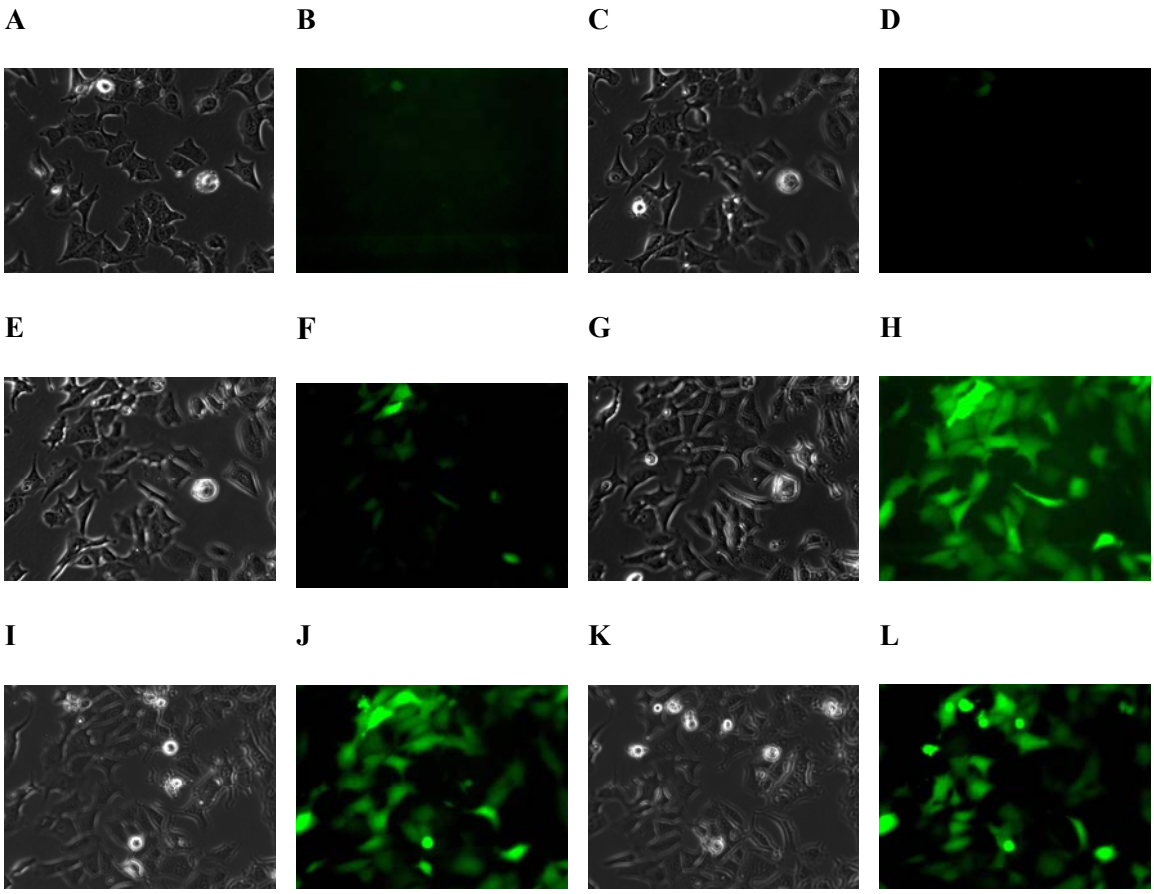


**Figure 4.** Phase and fluorescence images of H35 NF-κB-GFP reporter cells in response to 10ng/mL TNF-α stimulation. **A, C, E, G, I and K:** Phase contrast images of H35 NF-κB-GFP reporter cells at t=0, 4, 7, 14, 19 and 24hrs respectively. **B, D, F, H, J and L:** Fluorescence images of H35 NF-κB-GFP reporter cells at t=0, 4, 7, 14, 19 and 24hrs respectively.

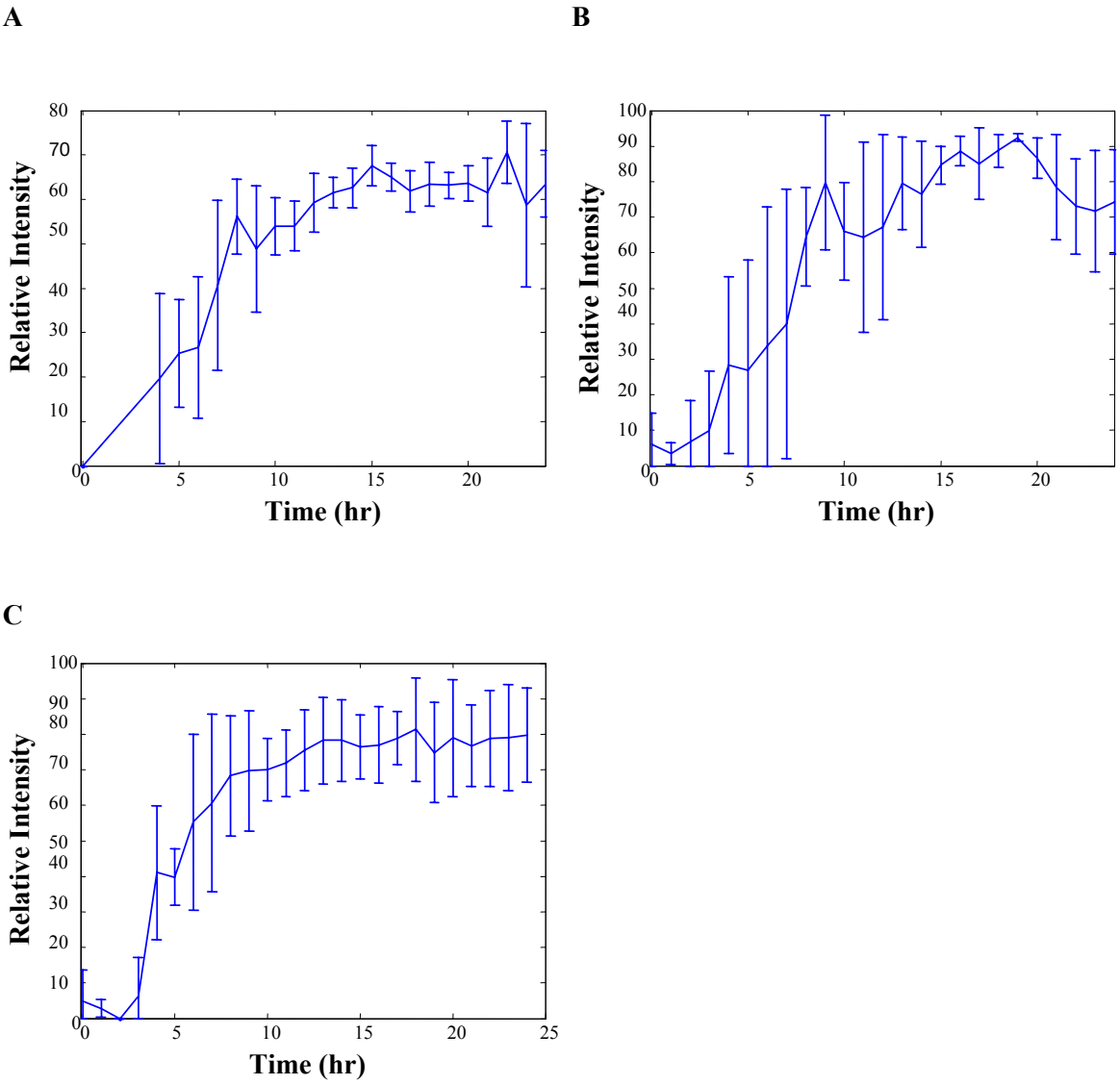


**Figure 5.** NF-κB-GFP expression profiles obtained by fluorescence microscopy and image analysis. Intensities are the average of the fluorescence intensities at three positions per TNF-α concentration. **A:** 2.5ng/mL stimulation TNF-α. **B:** 10ng/mL stimulation TNF-α. **C:** 25ng/mL stimulation TNF-α.

seeded in a 6-well plate at a density of approximately $5 \times 10^6$ cells/well in phenol red free DMEM. The fluorescence of H35 cells constitutively expressing GFP was monitored for 14 hours by fluorescence microscopy. The relative intensities of cells

constitutively expressing GFP were determined by image analysis. Figure 6 shows H35 cells constitutively expressing GFP. Over the duration of the analysis, GFP expression was found to be relatively constant, as shown in Figure 7. Comparison of expression profiles of NF-κB-GFP and constitutive GFP over the first 14 hours (Figures 5 and 7) shows that the fluorescence intensities obtained from TNF-α stimulation of NF-κB-GFP reporter cells are higher than those of constitutive GFP. Since image analysis parameters were maintained constant between these two data sets, the differences in fluorescence intensities are likely due to only GFP expression. Since GFP expression is driven in the constitutive GFP cell line by the native CMV promoter, and the NF-κB-GFP reporter cell line is under the control of a minimal promoter, one would expect higher fluorescence from the constitutive GFP cell line.

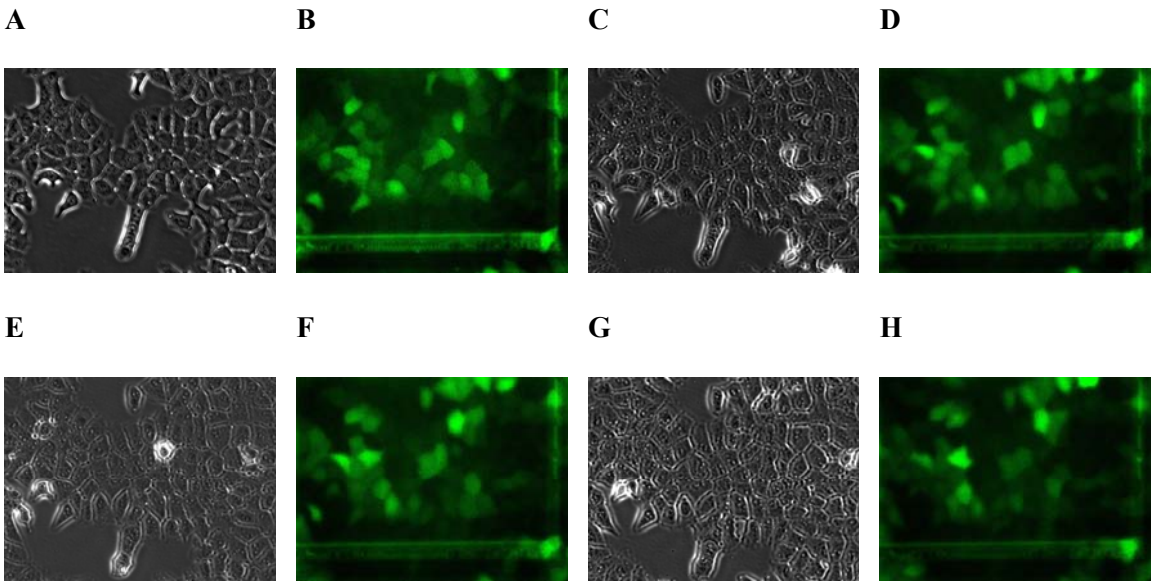


**Figure 6.** Phase and fluorescence images of H35 cells constitutively expressing GFP. **A, C, E and G:** Phase contrast image of H35 cells expressing constitutive GFP at t=1, 6, 9 and 14hrs respectively. **B, D, F and H:** Fluorescence images of H35 cells expressing constitutive GFP at t=1, 6, 9 and 14hrs respectively.

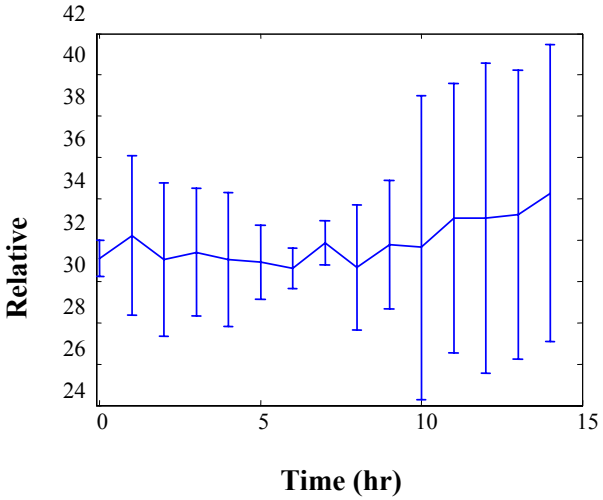


**Figure 7:** Profile of H35 cells constitutively expressing GFP over a 14 hour period. Intensities are the average of the fluorescence intensities at three positions per well.

**Determination of NF-κB Activation Profiles from GFP Reporter Profiles**

Personal contributions to this study were directed towards experimentally obtaining H35 NF-κB-GFP fluorescence data and proposing a model describing GFP transcription, translation, and modification. Other contributions were put forth by Zuyi Huang in Dr. Juergen Hahn's research group. It should be noted that other models and expression profiles given in this thesis are entirely based on the experimental H35 NF-κB-GFP fluorescence data and/or the model describing GFP expression.

GFP expression in H35 NF-κB-GFP reporter cells is induced upon NF-κB binding arising from TNF-α stimulation. Here we have sought to decouple GFP expression from NF-κB activation induced by TNF-α in order to obtain true NF-κB activation profiles by making use of models describing segments of the signaling events (Figure 2). The model $M_t$ describes the signaling events starting with TNF-α stimulation

and ending in fluorescence. The model $M_{GFP}$ depicts the transcription, translation and modification of GFP. $M_{NF\text{-}\kappa B}$ describes the events leading to NF-κB activation.

**Development of $M_t$ Model**

To the best of our knowledge there are no models available describing the TNF-α signaling pathway. Therefore, utilizing NF-κB-GFP reporter data, a mathematical model describing the relation between TNF-α stimulation and GFP fluorescence was extrapolated, which for convenience will be referred to as $M_t$ (Equation 2-3). Based on Figure 5B and C, it was assumed that the fluorescence profiles follow 1st order kinetics wit a time delay of approximately four hours. The mathematical model describing the relationship between TNF-α and green fluorescence was consequently developed as a 1st order ODE; and is based upon the output of green fluorescence intensities, a time delay and the input concentration of TNF-α.

$$I(t)-\alpha I(t-1)=\beta u(t-4) \tag{2}$$

$$u=\begin{cases} C \ \ if\ u\geq C, t>0 \\ u \ \ if\ 0\leq u<C, t>0 \end{cases} \tag{3}$$

$M_t$ is comprised of unknown constants $u$, $\alpha$ and $\beta$, where $u$ is a term used to specify the concentration of TNF-α, which reaches a maximum at an unspecified TNF-α saturation concentration $C$. The constants $\alpha$ and $\beta$ are parameters used to fit the extracted model to the experimental fluorescence intensity data of TNF-α induced expression of GFP in H35 NF-κB-GFP reporter cells. Constant identification can be performed by non-linear least squares analysis using the fluorescence intensity data and

the intensity output from $M_t$. Table 2 lists the values of the constants for $M_t$. The value of $u$ marks the saturation concentration of TNF-α, which was determined to be 3.2ng/mL.

**Table 2.** Numerical values of constants used for modeling signaling events of TNF-α stimulation to GFP fluorescence.

| Constant | Value | Unit |
|---|---|---|
| $\alpha$ | 0.7 | |
| $\beta$ | 6.4 | mL/ng |
| $u$ | 3.2 | ng/mL |

**Development of $M_{GFP}$**

A simple structured model for transient GFP expression for CHO cells has been described by Subramanian and Srienc (Subramanian and Srienc 1996). Using their model as a template, we formulated a detailed deterministic model, ($M_{GFP}$), to describe the transcriptional, translational, and posttranscriptional events involved in stable, single copy expression of green fluorescent protein in eukaryotic cells. The approach for generating the set of ODE's is based on mass balances, in which rates of synthesis and degradation for each species leads to the determination of species content. In the proposed model we assumed that the synthesis and degradation obey the same kinetics (Subramanian and Srienc 1996). It was also assumed that all transcripts in the model were subject to degradation (Iafolla and McMillen 2006).

For a stable system, the assumption made was that the DNA coding for GFP was integrated into the genome and not subject to degradation or dilution by growth. The rate of degradation for GFP plasmid content, $(p)$, is first order and follows steady state dynamics.

$$\frac{dp}{dt} = 0 \tag{4}$$

The accumulation of mRNA, $(m)$, is described by a synthesis term which is the product of the overall transcription rate, $(S_m)$, a factor, $(F)$, the concentration of inducer, and a degradation term with rate constant, $(D_m)$. $S_m$ is the overall transcription rate of mRNA. $S_m$ is a product of the velocity of RNA polymerase transcribing a DNA template, the length of the template, and the average number of RNA polymerase complexes on the template (Subramanian and Srienc 1996). The factor, $(F)$, is a parameter used to fit experimental data to the model. The inducer concentration term includes Michaelis-Menten type kinetics and accounts for the concentration of total inducer within a cellular system, $(C)$, (different from $C$ in $M_t$) and the concentration of inducer in the nucleus, $(C_i)$. In this way, the set of equations can be compared with models that employ a transciption factor as the inducer. In this case, $C$ can be assumed to be equivalent to any intracellular transcription factor protein levels. Since the accumulation of protein content is zero, the term $S_m F \frac{C_i}{C+C_i} p$ is a constant.

$$\frac{dm}{dt} = S_m F \frac{C_i}{C+C_i} p - D_m m \tag{5}$$

The intracellular accumulation of non-fluorescent protein transcribed, $(n)$, is given by the synthesis of mRNA and the overall translation rate, $(S_n)$. The overall translation rate is the product of the average velocity of the ribosomal complex translating a transcript, the length of the transcript and the average number of complexes

on the transcript (Subramanian and Srienc 1996). A degradation term modeled by first order kinetics with rate constant $D_n$ is also given. Since GFP requires a post-translational, oxygen dependent modification step to convert the nascent polypeptide into a fluorescent protein, a first order conversion term due to the fluorophore formation from nascent non-fluorescing protein with rate constant $S_f$ is furthermore described (Subramanian and Srienc 1996). Here mRNA degradation occurs in a single step. Ultimately, Equation 6 specifies the process of translating mRNA into early protein.

$$\frac{dn}{dt} = S_n m - D_n n - S_f n \tag{6}$$

The balance on fluorescing GFP, $(f)$, consists of a synthesis term due to the conversion of non-fluorescent protein to its fluorescing form and a degradation term with rate constant.

$$\frac{df}{dt} = S_f n - D_n f \tag{7}$$

Using literature, where available, the model was populated with known rate constants (Table 3). Where literature values could not be found, parameters were estimated to fit the experimental data. Differences in the half-lives of the transcripts and the translated products of GFP were expected to contribute to the difference in intracellular protein levels in stimulated cells (Subramanian and Srienc 1996). In this case, a four-hour half-life GFP variant was utilized for NF-κB-GFP reporter cells. Species content are expressed as macromolecules per cell.

**Table 3.** Numerical values for parameters used in the simulation of GFP expression in H35 cells.

| Model Parameters | Symbol | Unit | Value | Reference |
|---|---|---|---|---|
| Plasmid degradation rate | $D_p$ | $h^{-1}$ | 0.015 | (Subramanian and Srienc 1996) |
| Transcription rate | $S_m$ | per plasmid $h^{-1}$ | 3735 | (Subramanian and Srienc 1996) |
| mRNA degradation rate | $D_m$ | $h^{-1}$ | 2 | Estimated |
| Protein degradation rate | $D_n$ | $h^{-1}$ | 0.25 | Estimated |
| Fluorophore formation rate | $S_f$ | $h^{-1}$ | 3 | Estimated |
| Relational factor | $F$ | | 0.5263 | Estimated |
| Total cellular inducer concentration | $C$ | nM | 0.5 | Hahn and Huang, unpublished |
| Nuclear inducer concentration | $C_i$ | nM | 3.2 | Estimated |

The initial conditions of GFP production included the assumptions that the amount of mRNA, nascent non-fluorescing protein and fluorescent GFP were zero. The initial GFP plasmid copy number was assumed to be 5 since there are relatively few copies of GFP in the genome. Figure 8 below shows the expression profile of GFP as a step function generated from $M_{GFP}$. The profile shows that there is approximately a 30-minute time-delay followed by an increase of expression for 12 hours.

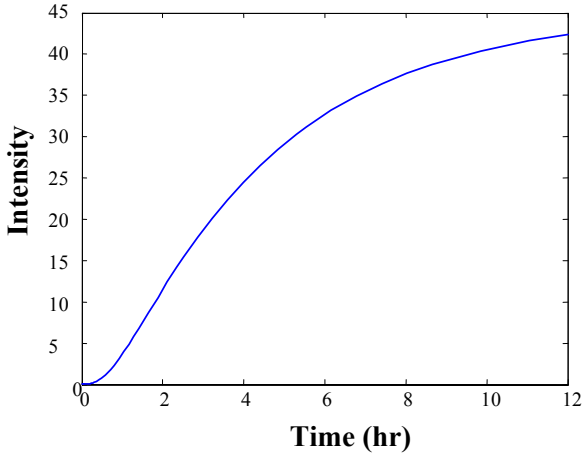


**Figure 8.** GFP expression simulated from the $M_{GFP}$ model describing GFP transcription, translation and modification.

### Extraction of NF-κB Dynamics

The $M_{GFP}$ model was used in conjunction with the $M_t$ model to extract NF-κB activation dynamics. To obtain NF-κB activation profiles, a mathematical model, namely $M_{NF\text{-}\kappa B}$, describing NF-κB activation was generated by comparing the proposed model, $M_{GFP}$, depicting GFP transcription, translation and modification, to $M_t$. Since both $M_{GFP}$ and $M_t$ are 1st order models, it was hypothesized that $M_{NF\text{-}KB}$ will also be a 1st order model. $M_{NF\text{-}\kappa B}$ was constructed as a simple transfer function by dividing $M_t$ by a constant. $M_{NF\text{-}\kappa B}$ contains unknown parameters $K_p$, $T_p$ and $T_d$ describing the static gain, time constant and time delay respectively. Since $M_t$ and $M_{GFP}$ are in the form of non-linear differential equations, $M_{NF\text{-}\kappa B}$ was transferred into a differential equation as a function of time using an inverse Laplace transform by assuming the initial concentrations of TNF-α and NF-

κB were equal to zero. The models for NF-κB activation as a transfer function and in its differential equation form along with initial conditions are given by Equations 8 and 9.

$$C_{NF-\kappa B} = \frac{K_p}{T_p s + 1} e^{-T_d s} \tag{8}$$

$$\frac{dC_{NF-\kappa B}}{dt} = -\frac{1}{T_p} C_{NF-\kappa B} + \frac{K_p}{T_p} u(t - T_d) \tag{9}$$

Combining $M_{GFP}$ and $M_{NF-\kappa B}$ elicits fluorescence intensities as an output for given TNF-α concentrations. $M_{GFP}$ and $M_{NF-\kappa B}$ together describe the relational events from TNF-α stimulation to GFP fluorescence. Since $M_t$ also describes the same pathway, given the same input concentrations of TNF-α, $M_t$ alone should generate the same intensity outputs as that of $M_{GFP}$ in combination with $M_{NF-\kappa B}$. Since the species in $M_{GFP}$ are given in units of molecules per cell and the variables in $M_t$ are given in units of fluorescence, the units in $M_{GFP}$ were converted to fluorescence intensity units by the following equation.

$$I = f \frac{\Delta I}{\Delta f} f = 2.4 \times 10^{-5} f \tag{10}$$

To unify the units of molecules per cell and fluorescence, parameters in $M_{NF-\kappa B}$ were set to have the similar intensities to that given by $M_t$. The fluorescence difference $\Delta f$ can be calculated by utilizing two different TNF-α concentrations in $M_{NF-\kappa B}$ to obtain the fluorescence outputs in $M_{GFP}$. The intensity difference $I$ can be calculated by utilizing the same TNF-α concentrations to the fluorescence outputs in $M_t$. In this case 2.5ng/mL and 10ng/mL of TNF-α were employed. The intensity

value $f$ obtained from $M_{GFP}$ in macromolecules per cells can then be transferred to the fluorescence intensity units.

Because the fluorescence intensity outputs generated by $M_{GFP}$ in conjunction with $M_{NF\text{-}\kappa B}$ are the same to those of the fluorescence intensity data, and since the parameters of $M_{NF\text{-}\kappa B}$ are unknown, comparison of the fluorescence intensity data to that of $M_{NF\text{-}\kappa B}$ in conjunction with $M_{GFP}$ were used to identify the unknown model parameters in $M_{NF\text{-}\kappa B}$ by non-linear least squares using the Levenberg-Marquardt method in MATLAB (Levenberg 1944; Marquardt 1963). The parameter values for $M_{NF\text{-}\kappa B}$ are listed in Table 4.

**Table 4.** Numerical values of parameters used in the simulation of NF-κB activation.

| Parameter | Value | Unit |
|---|---|---|
| $K_p$ | 0.9 | |
| $T_p$ | 0.4 | hr |
| $T_d$ | 1.6 | hr |

Following the identification of parameter values for $M_{NF\text{-}\kappa B}$, a time-dependent NF-κB activation profile was generated using $M_{NF\text{-}\kappa B}$ at the TNF-α saturation concentration and is shown in Figure 9. The NF-κB activation profile above shows a 90-minute time delay followed by a rapid increase in NF-κB activation. The intensity outputs from $M_{GFP}$ and $M_{NF\text{-}\kappa B}$ were compared to the fluorescence intensity data at each TNF-α concentration (Figure 10) to show how $M_{GFP}$ and $M_{NF\text{-}\kappa B}$ fit the experimental fluorescence data.

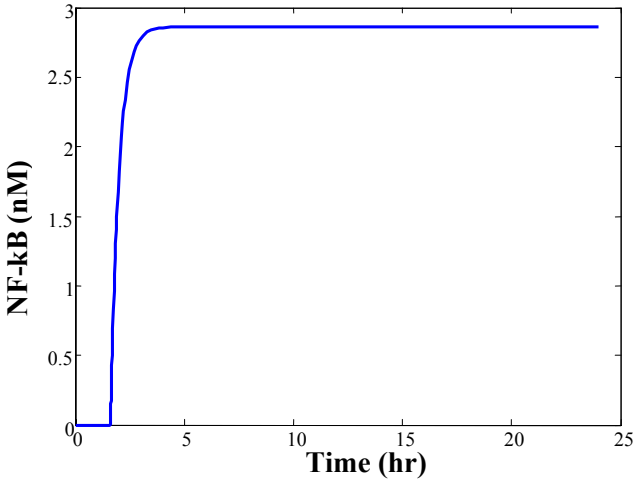


**Figure 9.** NF-κB activation profile. The profile was constructed for the saturation TNF-α concentration.

**A**

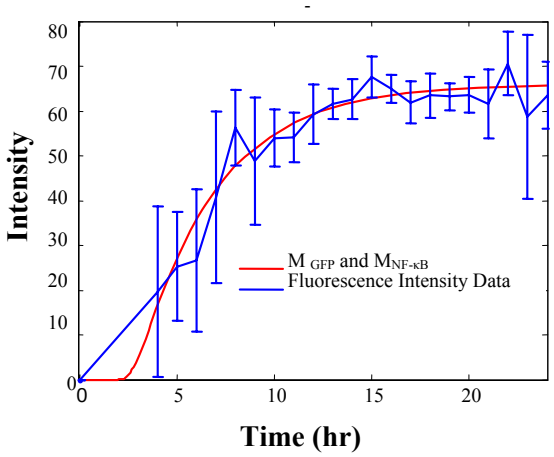


**B**

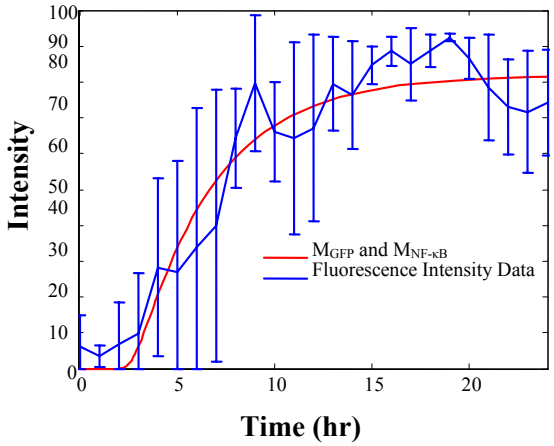


**C**

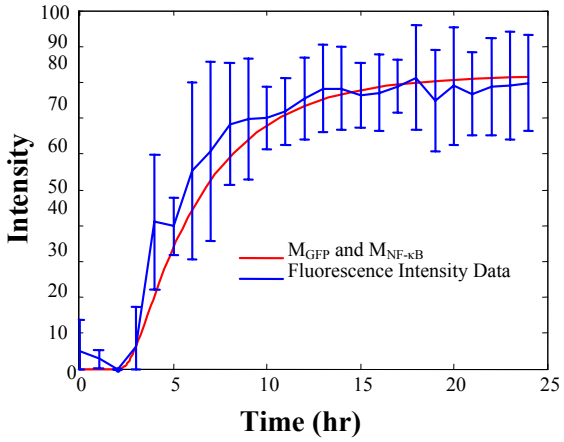


**Figure 10**: Comparison of $M_{GFP}$ and $M_{NF\text{-}\kappa B}$ to fluorescence intensity data**. A:** With 2.5ng/mL TNF-α stimulation. **B:** With 10ng/mL TNF-α stimulation. **C:** With 25ng/mL TNF-α stimulation.

# CHAPTER V

# SUMMARY AND FUTURE DIRECTIONS

## Summary

We have used mathematical modeling to determine NF-κB activation profiles from fluorescence profiles generated with H35 NF-κB-GFP reporter cells. H35 reporter cells that expressed GFP in response to NF-κB activation were used to determine fluorescence intensities and GFP expression profiles. Using intensity data from GFP reporter cells, a model representing TNF-α signaling and GFP production was extracted. A model describing regulatable transcription, translation and posttranslational modification of GFP was proposed. Utilizing this model in conjunction with the model depicting TNF-α and GFP expression, a third model describing NF-κB activation dynamics was constructed. NF-κB activation profiles were generated by simulation of the NF-κB activation model.

## Future Work

An assumption made in this study is that the proposed model representing regulatable GFP expression can describe the kinetics of GFP expression without verification. Since obtaining NF-κB activation profiles hinges on the utilization of this model, the NF-κB activation profiles provided in this study are presumed to be accurate without validation. Secondly, TNF-α can have pleiotropic effects that can directly or indirectly affect NF-κB activation and GFP expression. Therefore, it is necessary to rule out such effects and ascertain whether the GFP model is valid. This can be accomplished using a regulatable plasmid system, such as the Tet-On System (Clonetech, Mountain View CA). The Tet-

On system consists of two plasmids, the Tet-On vector (encoding for an rtTA protein) and the response vector, pRevTRE. In the presence of a chemical inducer (tetracycline), pTet-On expresses the reverse transcriptional activator (rtTA), which binds to TRE and activates transcription of GFP (or any reporter cloned in pRevTRE). In other words, the Tet-On system simulates transcription factor action in which the inducer, tetracycline, is functionally similar to TNF-α, and rtTA production from the Tet-On plasmid is similar to NF-κB activation. This type of expression system is useful since the addition of tetracycline directly induces rtTA expression without activation of other signaling pathways, and the resultant GFP will directly give GFP dynamics. Experimental dynamic profiles obtained from image analysis of the fluorescence response to various tetracycline concentrations and/or application of concentration fluxes over short durations of time (pulses) can lead to the validation of the proposed GFP model by comparing the fluorescence data to GFP model simulations.

In this study, a saturation concentration of TNF-α was determined. To verify this value, NF-κB-GFP reporter cells can be stimulated with other concentrations of TNF-α that are greater than or less than the determined saturation concentration. Applying a number of TNF-α stimulations to NF-κB-GFP reporter cells and obtaining the subsequent GFP profiles can also be used to substantiate $M_t$.

Microfluidic devices can futhermore be utilized to validate of $M_{GFP}$. The emergence of microfluidic devices has the potential to be utilized for the determination of gene expression profiles in single cells. Microfluidic devices are beneficial for expression profiling of reporter cells since it allows for rigorous control of induction and

concentration pulses. Modeling is especially benefitted by the use of microfluidic devices in that devices can lead to the determination of dynamic events on the single cell level, which may allow the construction models that represent a better depiction of signaling events. Verification of the proposed model by using the Tet-On GFP system in tandem with microfluidic devices can then lead to the extraction of other transcription factor activation profiles over various dynamic situations by mechanistic modeling performed in this study.

# REFERENCES

Barnes PJ, Karin K. 1997. Nuclear factor-κB-A pivotal transcription factor in chronic inflammatory diseases. N Engl J Med 36: 1066-1071.

Baumann H, Gauldie J. 1994. The acute phase response. Immunol Today 15: 74-80.

Chen FE, Ghosh G. 1999. Regulation of DNA binding by Rel/NF-kB transcription factors: Structural views. Oncogene 18: 6845-6852.

Ding GJF, Fischer PA, Boltz RC, Schmidt JA, Colaianne JJ, Gough A, Rubin RA, Miller DK. 1998. Characterization and quantitation of NF-κB nuclear translocation induced by interleukin-1 and tumor necrosis factor-α. J Biol Chem 273: 28897-28905.

Han Y, Brasier AR. 1997. Mechanism for biphasic RelA NF-kB1 nuclear translocation in tumor necrosis factor α-stimulated hepatocytes. J Biol Chem 272: 9825-9832.

Han Y, Weinman S, Boldogh I, Walker RK, Brasier AR. 1999. Tumor necrosis factor-α-inducible IκB proteolysis mediated by cytosolic m-calpain. J Biol Chem 274: 787-794.

Henkel T, Machleidt T, Alkalay I, Kronke M, Ben-Nerla Y, Baeuerie PA. 1993. Rapid proteolysis of IκB-alpha is necessary for activation of transcription factor NF-κB. Nature 365: 182-185.

Iafolla MAJ, McMillen DR. 2006. Extracting biochemical parameters for cellular modeling: A mean-field approach. J Phys Chem B 110: 22019-22028.

Jayaraman A, Yarmush ML, Roth CM. 2000. Dynamics of gene expression in rat hepatocytes under stress. Metab Eng 2: 239-251.

Jobin C, Holt L, Bradham CA, Streetz K, Brenner DA, Sartor RB. 1999. TNF receptor-associated factor-2 is involved in both IL-1β and TNF-α signalling cascades

leading to NF-κB activation of IL-8 expression in human intestinal epithelial cells. J Immunol 162: 4447-4454.

Levenberg K. 1944. A method for the solution of certain problems in least-squares. Quarterly Appl Math 2: 164-168.

Marquardt D. 1963. An algorithm for least-squares estimation of nonlinear parameters. SIAM J Appl Math 11: 431-441.

Moshage H. 1997. Cytokines and the hepatic acute phase response J Pathol 181: 257-266.

Ros JE, Schuetz JD, Gueken M, Streetz K, Moshage H, Kuipers F, Manns MP, Jansen PL, Trautwein C, Muller M. 2001. Induction of *Mdr1b* expression by tumor necrosis factor-α in rat liver cells is independent of p53 but requires NF-κB signaling. Hepatology 1425-1431.

Sanguinetti G, Lawrence ND, Rattray M. 2006. Probabilistic inference of transcription factor concentrations and gene-specific regulatory activities. Bioinformatics 22: 2775-2781.

Sass G, Chembade ND, Tiegs G. 2005. Tumer necrosis factor α (TNF)-TNF receptor 1-inducible cytoprotective proteins in the mouse liver: Relevance of suppressors of cytokine signaling. Biochem J 385: 537-544.

Siebenlist U, Franzoso G, Brown K. 1994. Structure, regulation and function of NF-κB. Annu Rev Cell Biol 10: 405-55.

Smyth MJ, Johnstone RW. 2000. Role of TNF in lymphocyte-mediated cytotoxicity. Micro Res and Tech 50: 196-208.

Stelling J. 2004. Mathmatical models in microbial systems biology. Curr Opin Microbiol 7: 513-518.

Subramanian S, Srienc F. 1996. Qualitative analysis of transient gene expression in mammalian cells using the green fluorescent protein. J Biotech 49: 137-151.

Thompson DM, King KR, Weider KJ, Toner M, Yarmush ML, Jayaraman A. 2004. Dynamic gene expression profiling using a microfabricated living cell array. Anal Chem 76: 4098-4103.

Tian B, Brasier AR. 2003. Identification of a nuclear factor κB-dependent gene network. Recent Prog Horm Res 58: 95-130.

Ullah M, Schmidt H, Cho K-H, Wolkenhauer O. 2006. Deterministic modelling and stochastic simulation of biochemical pathways using MATLAB. IEE Proc-Syst Biol 153: 53-59.

Wheelhouse NM, Chan Y-S, Gillies SE, Caldwell H, Ross JA, Harrison D, Prost S. 2003. TNF-α induced DNA damage in primary murine hepatocytes. Intern J of Mol Med 12: 889-894.

Wieder KJ, King KR, Thompson DM, Zia C, Yarmush ML, Jayaraman A. 2005. Optimization of reporter cells for expression profiling. Biomed Devices 7: 213-222.

Wokenhauer O, Ullah M, Wellstead P, Cho K-H. 2005. The dynamic systems approach to control and regulation of intracellular networks. FEBS Lett 579: 1846-1853.

Zambon A, Gervois P, Pauletto P, Fruchart J-C, Staels B. 2006. Modulation of hepatic inflammatory risk markers of cardiovascular diseases by PPAR-α activators clinical and experimental evidence. Arterioscler Thromb Vasc Biol 26: 977-986.

# VITA

Name: Allyson Marie Laible

Address: 2757 Mt. Borah Pl. Pocatello, ID 83201

Email Address: allyson0207@yahoo.com

Education: B.S. Chemistry. Seattle University, 2004